International Journal on Emerging Technologies **10**(4): 454-464(2019)

ISSN No. (Print): 0975-8364
ISSN No. (Online): 2249-3255

Multiple Clip conditions on Chemically Reacting Flow of MHD Jeffrey Fluid over Vertical surface in a Suspension of Brownian Motion and Thermophoresis

D. Manjula[1] and K. Jayalakshmi[2]
[1]Research Scholar, Department of Mathematics, JNTUA, Anantapur (Andhra Pradesh), India.
[2]Assistant Professor, Department of Mathematics, JNTUA College of engineering Anantapur (Andhra Pradesh), India.

(Corresponding author: D. Manjula)
(Received 02 September 2019, Revised 01 November 2019, Accepted 09 November 2019)
(Published by Research Trend, Website: www.researchtrend.net)

ABSTRACT: The current attempt focuses on comparative study of the Assisting and opposing Jeffrey fluid flow characteristics of chemically reacting and thermal radiated vertical exponential surface with multiple slip conditions at the boundary (velocity, thermal and diffusion). Further, thermophoresis, Brownian motion, magneto hydrodynamics, thermal radiation are also accounted. The flow governing equations remain altered toward ordinary differential equations (ODE's) through the aid of appropriate alterations. Runge-Kutta technique is acquired for the reliable and presentable results. The effect of different involved flow variables proceeding velocity, temperature in addition to deliberation as well as skin friction, Sherwood and Nusselt numbers are visualized in addition to discussed over graphs also tables. The foremost physical implication of the result is that the opposing flow is useful for the purpose of improving temperature distribution when compared to assisting flow. From this we can conclude that based on the situation we can use assisting or passive flow condition cases.

Keywords: Brownian motion, Vertical exponential surface, Thermophoresis, Multiple Slips, chemical reaction, Chemical reaction, Magneto hydro dynamic, Thermal radiation.

I. INTRODUCTION

Recently, the Boundary layer flow of extending surfaces has pulled in staggering attention due to a giant number of makes use of in industry and assembling frameworks. For delineation, numerous handy strategies regarding polymers envelop cooling of infinite strips expelled from a kick the bucket through drawing them through a tranquil liquid with the well-asked cooling framework and in this manner. The turning of filaments, Glass blowing, continual throwing of metals and non-oxide metals encompass the flow over an exponentially extending floor. During the assembling development of these surfaces, the combination gave from space is prolonged to arrive at the proper thickness. Finally, in perspective on reaching the top-grade total object, this sheet coagulates as it permits through the water/air-nicely-ventilated frameworks. In water solidifying frameworks, the incorporation of nanoparticles can be building up the cooling movement functionality and might likewise decrease the temporary time. There is an enormous literature on the border layer movementconcluded a extending surface, however we simply refer to few present related to present studies [1-14]. All these investigations are started with no-slip condition at the boundary, different slip conditions (Velocity, thermal and diffusion) individually, magnetic field, aligned magnetic field, thermal radiation, forced convection and rotation effects with various flow geometries such as linear surface, unsteady linear surface, plate, vertical plate, linear vertical surface, cone, vertical and wedge etc. All these examinations employ no-slip situation at the borderline.

Improving, as a way as possible in beautiful the exhibition of everyday warmth circulates befitted the best issue due to the low heat conductivity of the most broadly recognized beverages, as an instance, water, oil, and ethylene glycol blend. Since the nice and cozy conductivity of solids is often higher than that of fluids, adding debris to a standard liquid to accumulate its warmth move highlights turned into created. Among all factors of particles, for example, full scale, small scale, and nano, due to positive complexities within the weight drop through the framework or preserving the mixture homogeneous, nano-scaled particles have entranced extra thought. These modest particles are fairly close in size to the atoms of the bottom liquid and accordingly can be perceived as fairly strong interferences with slight gravitational settling over tremendous stretches of time. Invented duration "nanofluid" was initiated by Choi (1995) to draw attention to engineered colloids collected of nanoparticles detached in a base fluid. Subsequent the important investigation of this perception through a significant amount of investigation in this field has increased exponentially. In the meantime, theoretical investigations stood developed toward ideal the nanofluids performances. Up to now, the suggested replicas are two-fold; dispersion and homogeneous flow models. Buongiorno (2006) decided that the homogeneous fashions tend to below watching for the nanofluid heat transmission coefficient due to nanoparticle size, scattering result is clearly inconsequential. From this time ahead, Buongiorno built up a non-compulsory version to portray the odd convective warmth pass development in nanofluids and annihilates the insufficiencies of the homogeneous and

scattering models. He has taken seven slip structures, consisting of state of being inactive, Brownian dispersion, thermophoresis, liquid waste, diffusiophoresis, gravity, Magnus and bid that, of these seven, just Brownian dissemination and thermophoresis are large slip additives in nanofluids. In addition, Buongiorno showed that disturbance isn't always inspired by using nanoparticles. In light of this disclosure, he proposed a two-element 4-circumstance non-homogeneous concord version for convective automobiles in nanofluids. Later on, comprehensive survey on nanofluid through heat in addition to mass transfer applications is investigated by Pang *et al.,* [15]. There after the above mentioned model using with comprehensive survey was examined through [16-23].
Considering the above mentioned engineering and industrial applications of nanofluid, MHD, Radiation in the field of heating and cooling systems, the present research is supported out to explore the influence of multiple slip effects (Velocity, temperature and diffusion), thermal radiation, Thermophoresis also Brownian motion on MHD Jeffrey fluid flow concluded vertical exterior through chemical reaction. Numerical technique will be enforced to acquire reliable and presentable results.

II. MATHEMATICAL FORMULATION

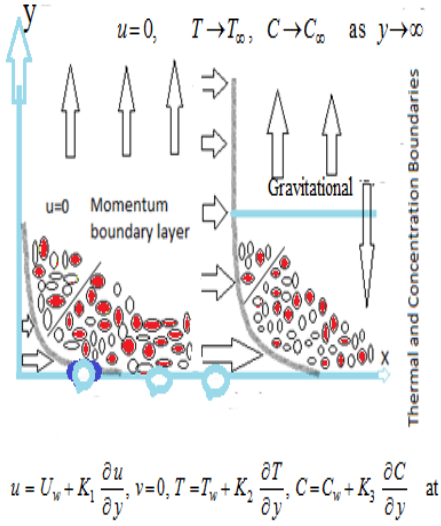

Fig. 1. The physical ideal of the flow formation.

$$u\frac{\partial u}{\partial x}+v\frac{\partial u}{\partial y}=\frac{\upsilon}{1+\lambda_1}\frac{\partial^2 u}{\partial y^2}+g\beta_T(T-T_\infty)$$
$$+g\beta_C(C-C_\infty)-\frac{\sigma B^2}{\rho}u+ \qquad (2)$$
$$\frac{\upsilon\lambda_2}{1+\lambda_1}\left(u\frac{\partial^3 u}{\partial x\partial y^2}+\frac{\partial u}{\partial y}\frac{\partial^2 u}{\partial x\partial y}-\frac{\partial u}{\partial x}\frac{\partial^2 u}{\partial y^2}+v\frac{\partial^3 u}{\partial y^3}\right)$$
$$u\frac{\partial T}{\partial x}+v\frac{\partial T}{\partial y}=\alpha\frac{\partial^2 T}{\partial y^2}-\frac{1}{\rho\ Cp}\frac{\partial q_r}{\partial y}$$
$$+\tau\left[D_B\frac{\partial T}{\partial y}\frac{\partial C}{\partial y}+\frac{D_T}{T_\infty}\left(\frac{\partial T}{\partial y}\right)^2\right] \qquad (3)$$

In this investigation, we considered a consistent II-dimensional MHD blended convection Jeffrey liquid over an exponentially radiated extending surface within the sight of Brownian motion also thermophoresis. To control the border coating phenomena, we also incorporated the multiple slips (velocity, thermal and diffusion slips) at the boundary. The x-organize is besides the extending sheet moreover the y-arrange is in use typical to the extending sheet. The page is extended vertically among velocity $U_w = u_0 \exp\left(\frac{X}{L}\right)$, where u_0 is a stable as well as L is the reference distance end to end. We besides supposed to facilitate the sheet have exterior warmth $T_w = T_\infty + T_0 \exp\left(\frac{X}{L}\right)$ as well as surface attentiveness $C_w = C_\infty + C_0 \exp\left(\frac{X}{L}\right)$, where T_0 as well as C_0 remain coefficients. T_∞ plus C_∞ are individually, the gratis stream hotness moreover consideration. The leading border coating equations in favor of the replica beneath deliberation are:

$$\frac{\partial u}{\partial x}+\frac{\partial v}{\partial y}=0 \qquad (1)$$

$$u\frac{\partial C}{\partial x}+v\frac{\partial C}{\partial y}=Dc\frac{\partial^2 C}{\partial y^2}-K_0(C-C_\infty) \qquad (4)$$

where u plus v exist the speed segments in the x along with y headings, individually. is the proportion of unwinding instance to hindrance occasion, is the impediment moment, T is liquid hotness, g is the gravitational force, C is liquid fixation, Dc, DB and DT is collection diffusivity (Concentration, Brownian diffusion and thermal diffusion), is the substance response speed steady, is kinematic consistency, is the radiative warmth transition, is liquid thickness. B is the compelling pasture which is implicit to exist $B = B_0 \exp\left(\frac{x}{L}\right)$ where, B_0 is a steady attractive field.
The equivalent border circumstances in favor of the flow representation are

$$\left.\begin{aligned} u &= U_w + K_1\frac{\partial u}{\partial y},\\ v &= 0\\ T &= T_w + K_2\frac{\partial T}{\partial y}\\ C &= C_w + K_3\frac{\partial C}{\partial y} \end{aligned}\right\} \text{at } y=0 \qquad (5)$$

$$u=0,\quad T\to T_\infty,\quad C\to C_\infty \quad \text{as} \quad y\to\infty \qquad (6)$$

where K_1, K_2 and K_3 speed, warm, moreover fixation slip factors. Not at all like the linearized Roseland guess, the nonlinear Roseland dissemination estimate is utilized beginning which single be able to acquire consequences in favor of together little moreover vast contrasts flanked by T_w also T_∞.

By using the Roseland diffusion estimate Roseland amongst additional researchers, the radiative warmth flux q_r is specified by:

$$q_r = -\frac{4\sigma^* T_\infty^3}{3K_s}\frac{\partial T^4}{\partial y} \quad (7)$$

Where σ* as well as K_S remain the Stefan-Boltzmann steady also the Roseland mean retention coefficient separately. We accept that the temperature contrasts inside the stream are adequately little with the goal that T might remain connected as a direct capacity of temperature T.

$$T^4 \approx 4T_\infty^3 T - 3T_\infty^3 \quad (8)$$

By means of Eqns. (7) in addition to (8) in the fourth expression of Eqn. (3) we develop:

$$\frac{\partial q_r}{\partial y} = -\frac{16\sigma^* T_\infty^3}{3K_s}\frac{\partial^2 T}{\partial y^2} \quad (9)$$

III. SIMILARITY TRANSFORMATIONS

We initiate the following comparison conversions:

$$\zeta = y\sqrt{\frac{u_0}{2\upsilon L}}\exp(x/2L), \quad u(\zeta) = u_0\exp(x/L)f'(\zeta)$$

$$v(\zeta) = \sqrt{\frac{u_0 v}{2L}}\exp(x/2L)\left[f(\zeta) + \zeta f'(\zeta)\right]$$

$$\theta(\zeta) = \frac{(T - T_\infty)}{(T_w - T_\infty)}, \quad \phi(\zeta) = \frac{(C - C_\infty)}{C_w - C_\infty} \quad (10)$$

Here ψ stays the stream/function such that $u = \frac{\partial \psi}{\partial y}$, $v = -\frac{\partial \psi}{\partial x}$ also stability equation is robotically fulfilled. Upon substitute the parallel variables hooked on Eqs. (2-4), we achieve the subsequent system of ODE:

$$f''' + \beta\left[ff'' + \tfrac{3}{2}(f'')^2 - \tfrac{1}{2}ff^{iv}\right] + (1+\lambda_1)\left[ff'' - 2(f')^2\right] \quad (11)$$
$$+(1+\lambda_1)\left[2\lambda_3\theta + 2\lambda_4\phi - M^2 f'\right] = 0$$

$$\left(\theta'' + \theta''\frac{4}{3}R\right) + 2\Pr\left[\frac{1}{2}f\theta' - f'\theta\right] + \quad (12)$$
$$\Pr\theta'\left[Nt\theta' + Nb\phi'\right] = 0$$

$$\phi'' + 2Le\left[\frac{1}{2}f\phi' - f'\phi - Kr\,\phi\right] + \frac{Nt}{Nb}\theta'' = 0 \quad (13)$$

The equivalent boundary circumstances to the distorted equations are:

$$f = 0, \quad f' = 1 + A f'', \quad \theta = 1 + B\theta', \quad \phi = 1 + D\phi'$$

at $\zeta = 0$ and $f' \to 0, \quad f'' \to 0, \quad \theta \to 0, \quad \phi \to 0$ as $\zeta \to \infty$ (14)

where $A = K_1\sqrt{\frac{u_0}{2\upsilon L}}\exp\left(\frac{x}{2L}\right)$, $B = K_2\sqrt{\frac{u_0}{2\upsilon L}}\exp\left(\frac{x}{2L}\right)$ and $D = K_3\sqrt{\frac{u_0}{2\upsilon L}}\exp\left(\frac{x}{2L}\right)$ represent the velocity, thermal as well as solute slip limitations

$$Nb = \frac{D_B(C_w - C_\infty)(\rho c_p)_p}{\upsilon(\rho c_p)_f}$$

$$Nt = \frac{D_T(T_w - T_\infty)(\rho c_p)_p}{\upsilon(\rho c_p)_f}, \; Le = \frac{\upsilon}{D_B}$$

motion and thermophoresis and Lewis numbers respectively.

At this point, major signifies separation through respect to ζ, $\beta = u_0\lambda_2/L\exp(x/L)$ is the Deborah figure, $\lambda_3 = g\beta_T\exp(-2x/L)\upsilon L(T_w - T_\infty)$ is the thermal buoyancy restriction, $M^2 = \sigma B_0^2 u_0/\rho\exp(2x/L)$ is the attractive parameter, $\lambda_4 = g\beta_T\exp(-2x/L)\upsilon L(C_w - C_\infty)$ is the solutal buoyancy/limitation, $R = 4\sigma^* T_\infty^3/k\,k^*$ is the thermal radiation restriction, $\Pr = \upsilon/\alpha$ is the Prandtl figure, $Sc = \upsilon/Dc$ is the Schmidt integer, as well as $Kr = K_0\exp(-x/L)$ is the chemical-response/parameter.

IV. LOCAL SKIN FRICTION, NUSSELT/NUMBER ALSO SHERWOOD NUMBER

The parameters of physical concentration in favor of the present difficulty remain the restricted skin resistance coefficient C_f, the local-Nusselt-number Nu_x as well as local Sherwood figure Sh_x which are definite as:

$$\frac{1}{2}Cf_x\,\mathrm{Re}_x^{1/2} = \frac{1}{1+\lambda_1}f''(0)$$
$$\frac{1}{2}Nu_x\,\mathrm{Re}_x^{-1/2} = -\left(1 + \frac{4}{3}R\right)\theta'(0) \text{ and } \frac{1}{2}Sh_x\,\mathrm{Re}_x^{-1/2} = -\phi'(0) \quad (15)$$

Here the warmth move rate along with local Sherwood digit at the exterior correspondingly on behalf of a variety of standards of the parameters is obtainable in Table 1 and 2.

V. RESULTS AND DISCUSSION

In imperative to attain a durable support of the physical ideal, the numerical answers on behalf of the flow physical properties like speed, temperature in addition to deliberation fields remain demonstrated graphically on behalf of dissimilar limitations of the magnetic field, Eckert number, Brownian motion, thermophoresis, thermal radiation also chemical response, Brownian motion, thermophoresis parameters appearing in the problem. Furthermore, illustrative outcomes on behalf of the skin-friction constant, local Nusselt also Sherwood statistics remain demonstrating the effect of innumerable physical limitations of the flow remain verified through tables on behalf of mutually opposing also assisting flow cases. Aimed at numerical clarifications we consume selected the non-dimensional limitation values as K = 0.5; B=0.2; D = 0.2; Le = 0.3; $\beta = 0.2; Nt = 0.2; Nb = 0.3,$ R = 0.5; Kr = 0.2; M=0.5; Pr=2; $\lambda_1 = 0.3.$ These numeric values endure preserved as common in entire study apart beginning the alterations in the compatible figures also tables. In this study graphs displays the Solid lines represents the opposite flow case also dashed lines represents the helping flow cases respectively.

Figs. 2 and 3 speculate the effect of thermophoresis on temperature in addition to concentration fields on behalf

of together opposing also assisting flow cases. As increasing values of *Nt* improves the thermal and concentration boundary coatings. In common as raising standards of *Nt* internal thermal diffusion in the flow owing to this we saw improvement in both hotness in addition to attentiveness fields. It is interesting to indication that the concentration field showed mixed behavior in the flow, as increasing opposing force automatically depreciates the diffusion of the particles. The effects of *Nb* on temperature and deliberation fields are plotted in Figs. 4 and 5. It is found that the temperature encourages also attentiveness reduces in the mutually the opposing also assisting flow cases. But it is clear starting the figures that the temperature distribution is less in assisting flow case when related to opposing flow case. Fig. 6 demonstrations the possession of chemical response on concentration field on behalf of mutually the assisting as well as opposing flow belongings. The chemical reaction suppresses the concentration boundary, this is due to the interfacial mass disturbance in the flow. The concentration distribution is more in similar flow related to assisting flow case. The thermal radiation on velocity, temperature also concentration fields are shown in Figs. 7 to 9. Thermal radiation improves the temperature, concentration and velocity fields. As we expected rising in thermal radiation creates warmth energy into the flow this assistance to encourages the temperature also velocity field. Interestingly, we found the thermal also diffusion borderline layer distribution is higher in opposing flow case.

The influence of λ_1 is on velocity, temperature in addition to concentration profiles are displayed in Figs. 10 to 12. The temperature and concentration fields remain enhanced rising values of λ_1, whereas velocity profiles are showed mixed performance in the flow. The Figs. 13 and 14 shows the decrement in temperature also concentration profiles on behalf of mutually the supporting also opposing flow cases in the occurrence of Deborah number. The opposite flow case has higher distribution compared to assisting flow with existence of Deborah number. The velocity slip on temperature, velocity as well as concentration fields on behalf of mutually the assisting also opposing flow cases in Figs. 15-17. The temperature and concentration field are boosted and reduced the velocity profiles. As we expected when we increase the velocity slip at the boundary the flow stick to the flow due to velocity boundary is reduced. Figs. 18 and 19 show the possession of thermal slip at the boundary on temperature and concentration fields for both the assisting and opposing flow situations. When we incorporate thermal slip at the boundary it sticks the thermal boundary due to this, we saw decrement in temperature and concentration boundaries. Far away from the boundary the influence of thermal slip is more in opposing flow. The diffusion slip on concentration is shown in Fig. 20. It is clear that as rising diffusion slip generates sudden jump at the surface due to this, we saw reduction in concentration boundary layer. Figs. 21-23 shows that the effect of *M* on temperature, velocity and concentration profiles, through these graph we analyzed that the effect of magnetic field increases the temperature also reduced the velocity profiles of both assisting and opposing flow boundary layers. Beginning these we can determine that the temperature and concentration distribution are higher in opposing flow case related to supporting flow case. Commencing this study, we container able to determine that for advanced temperature distribution we can use opposing flow.

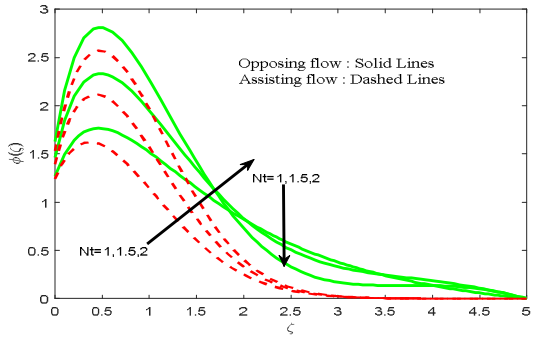

Fig. 2. Concentration profiles on behalf of dissimilar values of *Nt*.

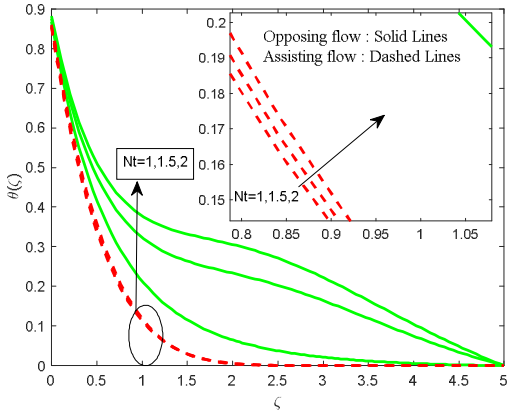

Fig. 3. Temperature profiles on behalf of altered values of *Nt*.

From Table 2 one can notice the variation in Skin $\left(\frac{1}{2}C_{fx}\,\mathrm{Re}_x^{1/2}\right)$, Nusselt $\left(\frac{1}{2}Nu_x\,\mathrm{Re}_x^{-1/2}\right)$ and Sherwood number $\left(\frac{1}{2}Sh_x\,\mathrm{Re}_x^{-1/2}\right)$ for different values of physical parameters for supporting flow Condition alsodisparate flow Condition. It is detected that $\left(\frac{1}{2}C_{fx}\,\mathrm{Re}_x^{1/2}\right)$ is decreasing function for improvement in $Nt, R, Nb, \lambda_1, \beta, A$ and M and increasing function for improvement in *Kr*, *B* and *D*. Confined Nusselt number $\left(\frac{1}{2}Nu_x\,\mathrm{Re}_x^{-1/2}\right)$ reductions through rising values of $Nt, Nb, Kr, \lambda_1, A, D$ and *M*, whereas $\left(\frac{1}{2}Nu_x\,\mathrm{Re}_x^{-1/2}\right)$ improves with improvement in *R*, β and *B*. It is similarly noticed that the friction factor also heats transfer rates remain more in assisting flow case related to opposing flow case.

Table 3 portrays the variation in Sherwood number $\left(\frac{1}{2}Sh_x\,\mathrm{Re}_x^{-1/2}\right)$ on behalf of dissimilar values of physical parameters for supporting in addition to opposing flow

cases. The Sherwood number $\left(\frac{1}{2}Sh_x \mathrm{Re}_x^{-1/2}\right)$ performance is increasing function for improvement in Kr, B, β and *Nb*, whereas the Sherwood number $\left(\frac{1}{2}Sh_x \mathrm{Re}_x^{-1/2}\right)$ depreciates for the rising values of Nt, M, A, D, λ_1.

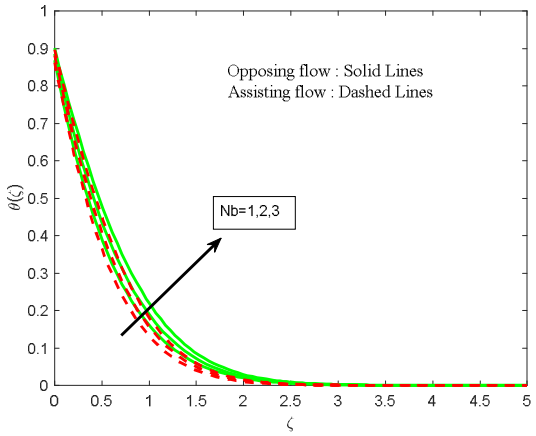

Fig. 4. Temperature profiles for changed standards of *Nb*.

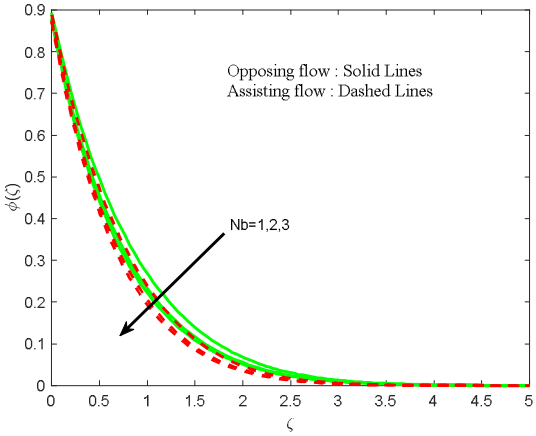

Fig. 5. Concentration profiles aimed at dissimilar values of *Nb*.

At the end, it is very clear that the mass transmission rate is advanced in opposing flow case related assisting flow. Depends on the industry perspective we can choose either opposing or assisting flow cases.

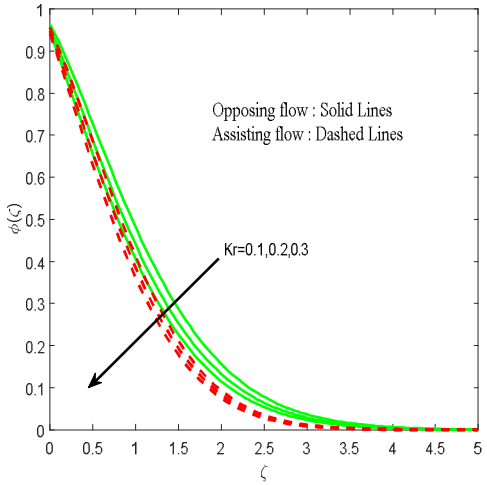

Fig. 6. Concentration profiles for changed values of *Kr*.

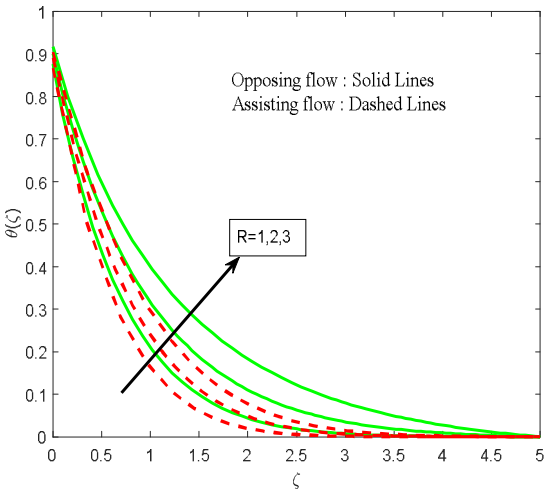

Fig. 7. Temperature profiles for changed standards of *R*.

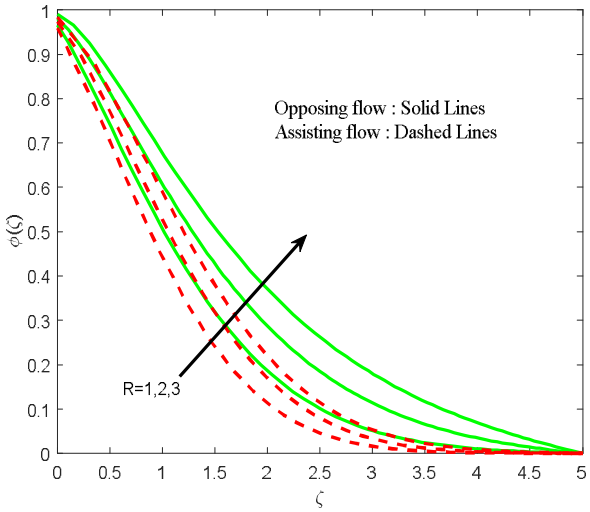

Fig. 8. Concentration profiles for changed values of *R*.

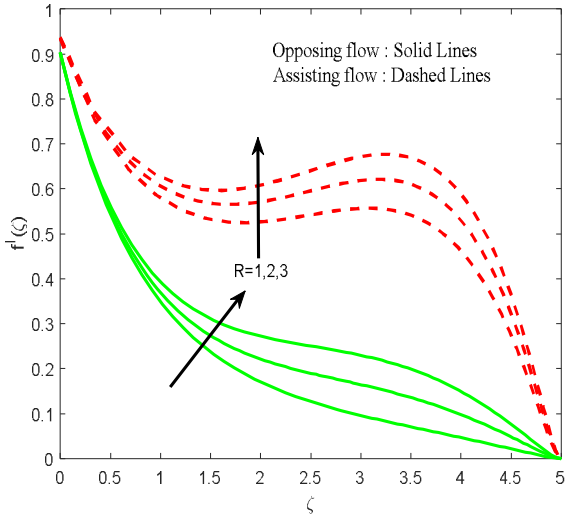

Fig. 9. Velocity profiles for altered values of *R*.

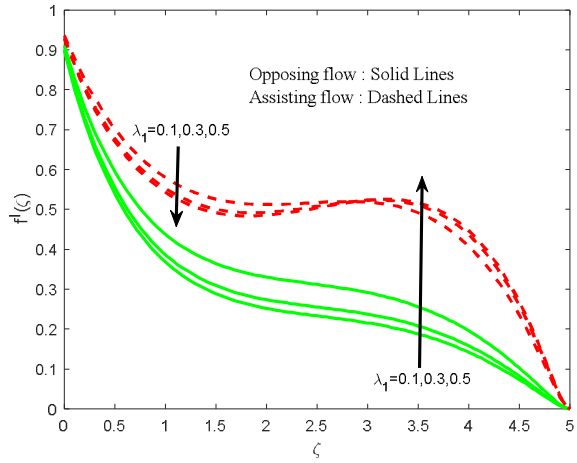

Fig. 10. Velocity profiles for changed values of λ_1.

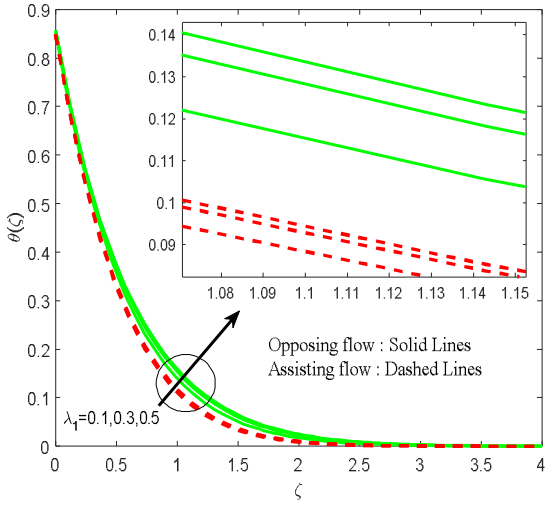

Fig.11. Temperature profiles on behalf of dissimilar values of λ_1.

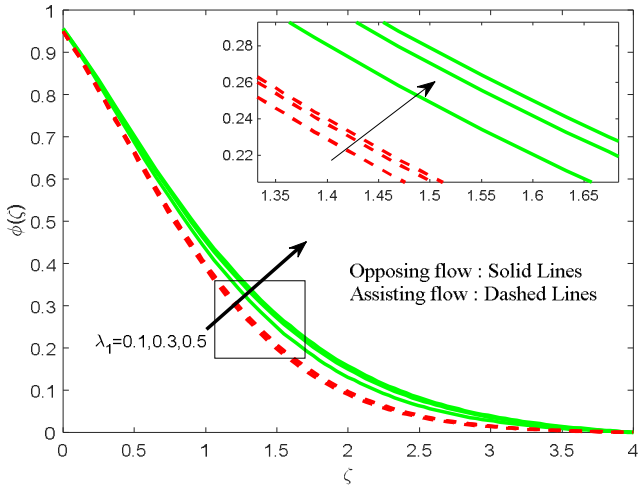

Fig.12. Concentration profiles for diverse values of λ_1.

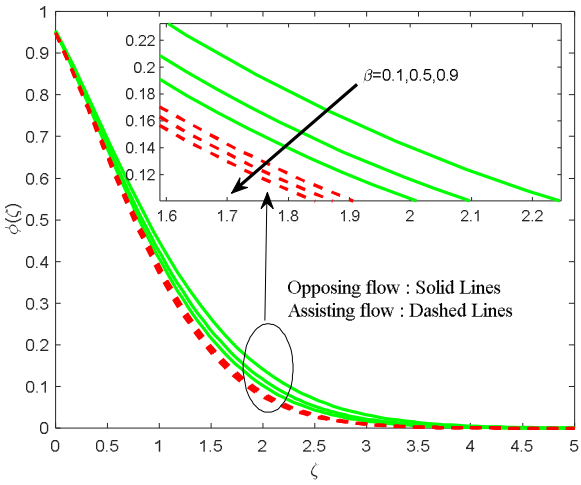

Fig.13. Concentration profiles for different values of β.

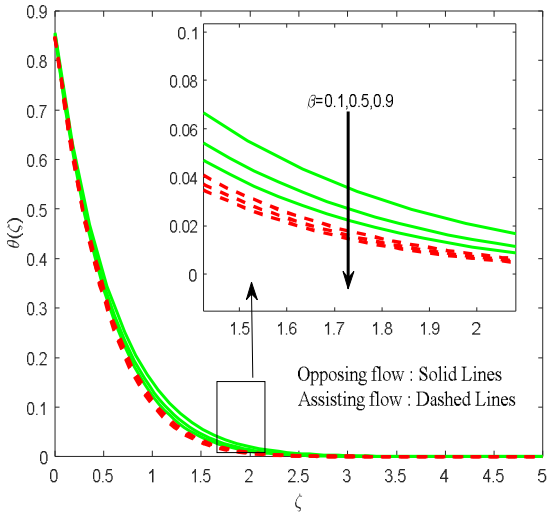

Fig.14. Temperature profiles for different values of β.

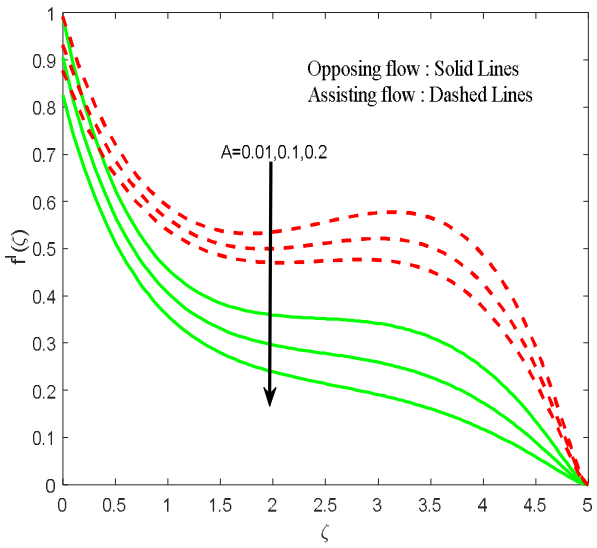

Fig.15. Velocity profiles for different values of *A*.

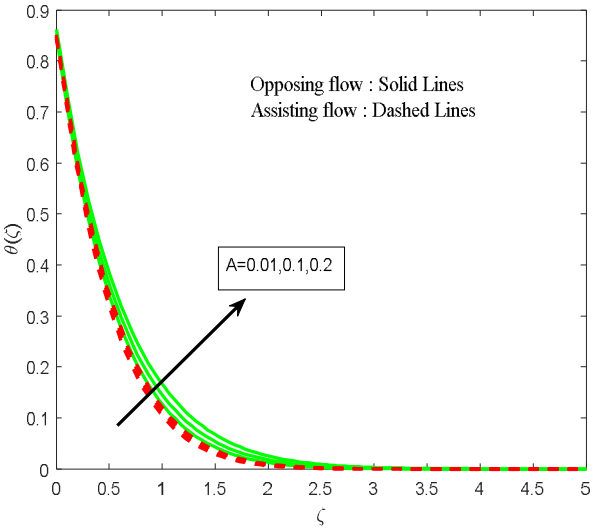

Fig.16. Temperature profiles for different values of *A*.

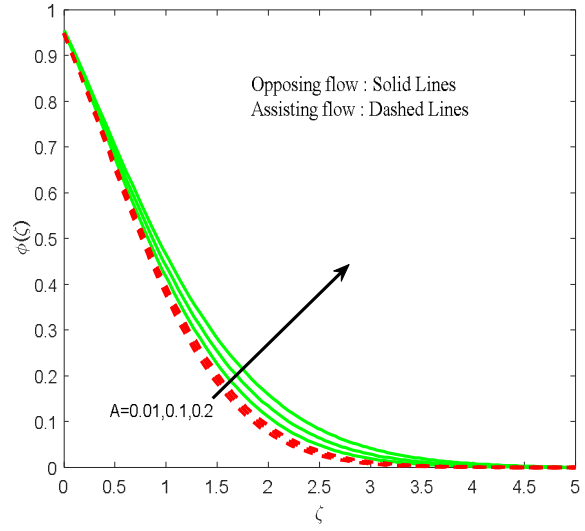

Fig.17. Concentration profiles for different values of *A*.

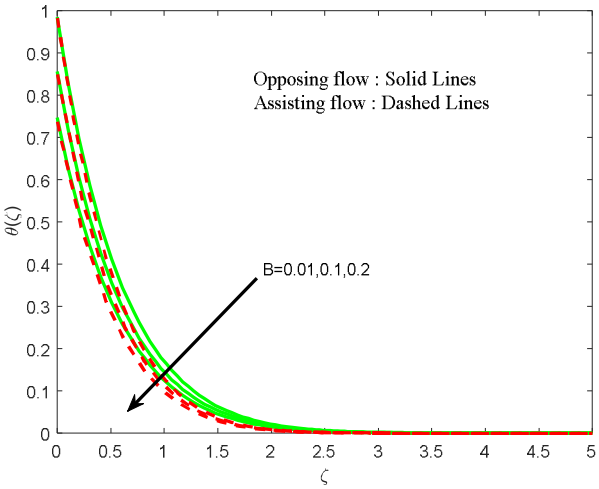

Fig.18. Temperature profiles for different values of *B*.

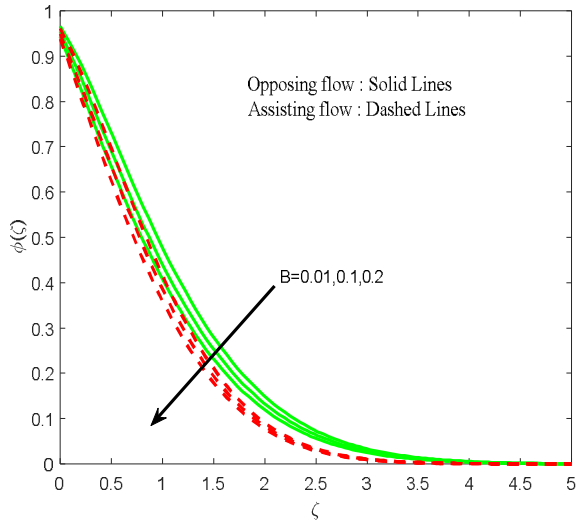

Fig.19. Concentration profiles for different values of *B*.

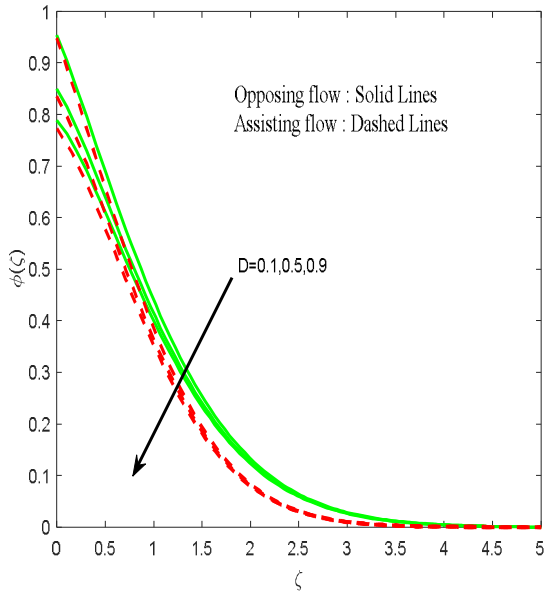

Fig. 20. Concentration profiles for different values of *D*.

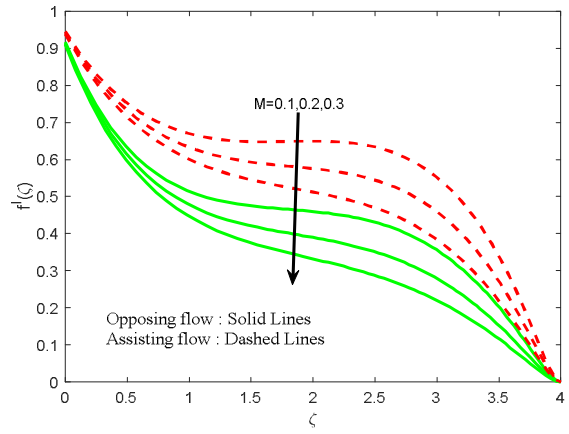

Fig. 21. Velocity profiles for different values of *M*.

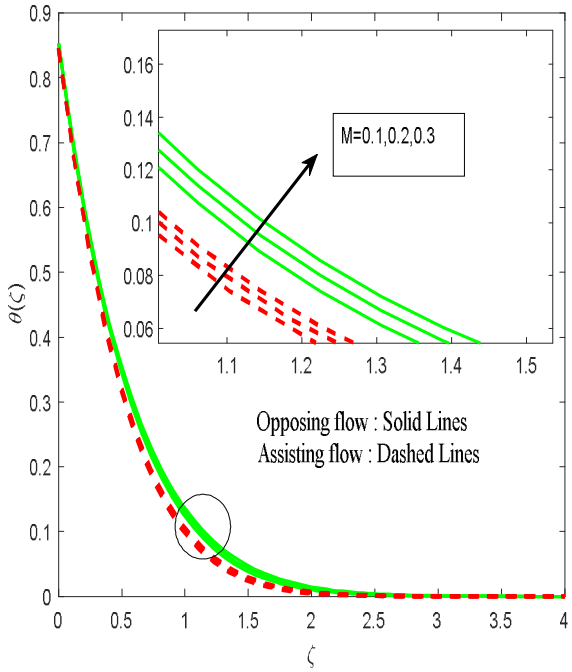

Fig. 22. Temperature profiles for different values of *M*.

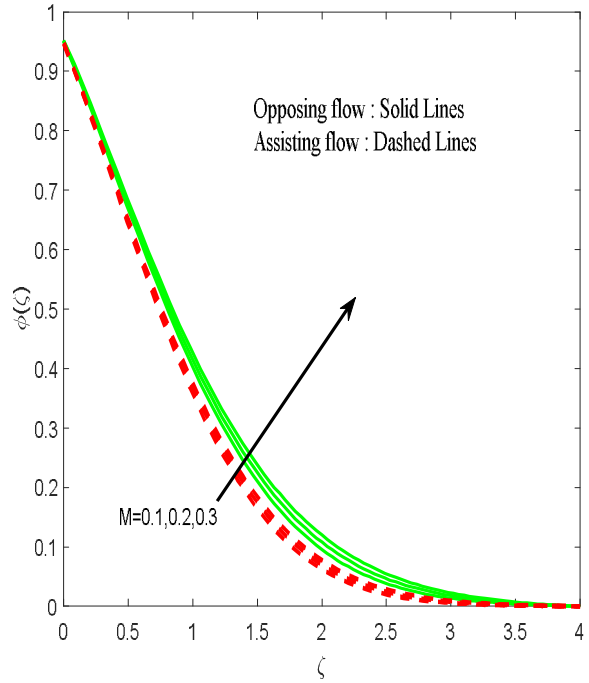

Fig. 23. Concentration profiles for different values of *M*.

Table 1: The variations in Skin $\left(\frac{1}{2}C_{fx}\,\mathrm{Re}_x^{1/2}\right)$ and Nusselt $\left(\frac{1}{2}Nu_x\,\mathrm{Re}_x^{-1/2}\right)$ for mutually opposite also supporting flow cases through different values of physical parameters.

Nt	*Nb*	*Kr*	*R*	λ_1	β	*A*	*B*	*D*	*M*	$\left(\frac{1}{2}C_{fx}\,\mathrm{Re}_x^{1/2}\right)$		$\left(\frac{1}{2}Nu_x\,\mathrm{Re}_x^{-1/2}\right)$	
										Opposing flow	Assisting flow	Opposing flow	Assisting flow
1										-0.301728	-0.163568	2.222849	2.449807
1.5										-0.312741	-0.142243	2.066004	2.388980
2										-0.321053	-0.122619	1.969604	2.324797
	1									-0.276771	-0.207280	2.196794	2.289864
	2									-0.276839	-0.207118	1.910428	1.989963
	3									-0.277400	-0.206002	1.660618	1.729567
		0.1								-0.280643	-0.200208	2.415129	2.540361
		0.2								-0.279900	-0.201320	2.411489	2.533557
		0.3								-0.279263	-0.202331	2.408291	2.527391
			1							-0.282281	-0.196893	2.898243	3.096371

			2							-0.285745	-0.190651	3.630126	4.019580
			3							-0.288253	-0.186274	4.155142	4.789904
				0.1						-0.261825	-0.189810	2.440027	2.548016
				0.3						-0.291182	-0.208436	2.393071	2.524616
				0.5						-0.301933	-0.215167	2.375021	2.516164
					0.1					-0.265266	-0.190100	2.397134	2.526714
					0.5					-0.318821	-0.232237	2.449040	2.552086
					0.9					-0.361872	-0.268210	2.488240	2.572455
						0.01				-0.309431	-0.226227	2.520814	2.600112
						0.1				-0.279900	-0.201320	2.411489	2.533557
						0.2				-0.253641	-0.179345	2.300248	2.471910
							0.01			-0.282229	-0.196663	2.760130	2.936175
							0.1			-0.279900	-0.201320	2.411489	2.533557
							0.2			-0.277928	-0.205199	2.112736	2.198664
								0.1		-0.279900	-0.201320	2.411489	2.533557
								0.5		-0.278499	-0.204226	2.425916	2.543599
								0.9		-0.277698	-0.205839	2.434187	2.549157
									0.1	-0.247063	-0.163990	2.476943	2.590627
									0.2	-0.256404	-0.174565	2.457838	2.574008
									0.3	-0.265003	-0.184381	2.439971	2.558382

Table2: The variations in Sherwood number $\left(\frac{1}{2}Sh_x \,\mathrm{Re}_x^{-1/2}\right)$ for mutually the opposing also assisting flow belongings with dissimilar values of physical limitations.

Nt	*Nb*	*Kr*	*R*	λ_1	β	*A*	*B*	*D*	*M*	$\left(\frac{1}{2}Sh_x \,\mathrm{Re}_x^{-1/2}\right)$		Time taken for execution in sec	
										Opposing Flow	**Assisting Flow**	**Opposing Flow**	**Assisting Flow**
1										-2.397284	-2.705221	3.761370	3.396307
1.5										-3.948683	-4.590217		
2										-5.299070	-6.288903		
	1									1.118654	1.067928	3.746389	2.628030
	2									1.246305	1.194185		
	3									1.287488	1.233319		
		0.1								0.433289	0.363150	2.988183	2.159899
		0.2								0.514064	0.460139		
		0.3								0.589379	0.547173		
			1							0.405300	0.346599	2.869979	2.287771
			2							0.260399	0.195012		
			3							0.164055	0.096275		
				0.1						0.519186	0.471817	2.810792	2.003089
				0.3						0.510951	0.452570		
				0.5						0.508047	0.445112		
					0.1					0.511647	0.453128	3.154764	2.202567
					0.5					0.520981	0.477383		
					0.9					0.528705	0.494149		
						0.01				0.521097	0.476753	2.861378	2.061753
						0.1				0.514064	0.460139		
						0.2				0.508109	0.444025		
							0.01			0.389727	0.339260	3.258733	2.266307
							0.1			0.514064	0.460139		
							0.2			0.617980	0.563371		
								0.1		0.514064	0.460139	2.949849	2.022818
								0.5		0.329708	0.301470		
								0.9		0.227742	0.210591		
									0.1	0.543483	0.497429	2.628673	1.915333
									0.2	0.533636	0.485281		
									0.3	0.524405	0.474076		

Table 3: Validation of present results with already available results under limited case.

β	λ_1	λ_3	M	R	A	B	D	Shateyi and Marewo [23]		Present results	
								$f''(0)$	$\phi'(0)$	$f''(0)$	$\phi'(0)$
0	0.1	0.5	1	1	0	0	0	4.67874	0.7862	4.67874	0.7862
2								2.66663	0.8121	2.66663	0.8121
	0							2.2398	0.8268	2.2398	0.8268
	3							4.3954	0.7875	4.3954	0.7875
		0						2.7597	0.8002	2.7597	0.8002
		1						2.3238	0.8342	2.3238	0.8342
			0					0.4249	0.9335	0.4249	0.9335
			2					1.6273	0.8599	1.6273	0.8599
				1				0.8077	0.9083	0.8077	0.9083
				3				0.8365	0.9028	0.8365	0.9028
					0			4.67874	0.7862	4.67874	0.7862
					0.2			3.8695	0.7862	4.67874	0.7862
						0		4.67874	0.7862	4.67874	0.7862
						0.3		4.3541	0.7862	4.67874	0.7862
							0	4.67874	0.7862	4.67874	0.7862
							0.5	4.67874	0.6754	4.67874	0.7862

VI. CONCLUDING REMARKS

The current attempt focuses on comparative study of the Assisting and opposing Jeffrey fluid flow characteristics of chemically reacting and thermal radiated vertical exponential surface with multiple slip conditions at the boundary (velocity, thermal and diffusion). Further, thermophoresis, Brownian motion, magneto hydrodynamics, thermal radiation are also accounted. The flow governing equations remain converted to ordinary differential equations (ODE's) through the aid of appropriate alterations. Runge-Kutta technique is acquired for the reliable and presentable results. The effect of numerous involved flow variables on velocity, temperature alsoattentiveness as well as skin friction, Sherwood and Nusselt statisticsremain visualized and discussed through graphs and tables. Founded on the current research the subsequent observations are made:

1. The foremost physical implication of the result is that the opposing flow is useful for the purpose of improving temperature distribution when compared to assisting flow.From this we can conclude that based on the situation we can use assisting or passive flow condition cases.
2. The rate of heat transmission is advanced in helping flow condition related to disparate flow conditions whereas skin friction and Sherwood numbers are quite opposite to that behavior. From this it is clear that depending on the situation we select the assisting or opposing flow conditions.
3. The temperature distribution is higher in opposing flow condition when compared to assisting flow condition. From above two results help us to conclude the based on the industrial need we can either assisting flow or opposing flow situations.
4. Due to high in pressure in opposing force the time take for the exaction is more time compared to assisting flow case.
5. The multiple slip conditions are useful for controlling the flow behavior and heat transport phenomena. The slip condition influence is lesser in assisting flow compared to opposing flow case.

FUTURE SCOPE

Future studies may consider melting surface and different non-Newtonian working fluids.

ACKNOWLEDGEMENTS

The authors are grateful to the reviewers for their comments which have served to improve the article

REFERENCES

[1]. Howarth, L. CXLIV. The boundary layer in three-dimensional flow. —Part II. The flow near a stagnation point. *The London, Edinburgh, and Dublin Philosophical Magazine and Journal of Science*, 195142(335), 1433-1440.

[2]. Hayat, T., Shehzad, S.A., Qasim, M. and Obaidat, S., Radiative flow of Jeffery fluid in a porous medium with power law heat flux and heat source. *Nuclear Engineering and Design*, 2012, Vol. *243*, pp.15-19.

[3].Turkyilmazoglu M. Multiple solutions of heat and mass transfer of MHD slip flow for the viscoelastic fluid

over a stretching sheet. *International Journal of Thermal Sciences.* 2011 Nov 1; *50*(11): 2264-76.
[4].Swain I, Mishra SR, Pattanayak HB. Flow over exponentially stretching sheet through porous medium with heat source/sink. *Journal of Engineering, Hindawi*. Vol . 2015, Pp 7.
[5].Sarkar J, Ghosh P, Adil A. A review on hybrid nanofluids: recent research, development and applications. *Renewable and Sustainable Energy Reviews*. 2015 Mar 1; Vol. *43*: 164-77.
[6]. T. Hayat, A. Shafiq, A. Alsaedi, and S. A. Shahzad. Vol. *37*: Issue no. 2, 193-208 (2016). Hayat T, Shafiq A, Alsaedi A, Shahzad SA. Unsteady MHD flow over exponentially stretching sheet with slip conditions. *Applied Mathematics and Mechanics.* 2016 Feb 1; *37*(2): 193-208.
[7]. Saritha, K., & Palaniammal, P. (2018). MHD Viscous Cassonfluid Flow in the Presence of a Temperature Gradient Dependent Heat Sink With Prescribed Heat And Mass Flux. *Frontiers in Heat and Mass Transfer (FHMT)*, *10*.
[8]. K.L. Hsiao, (2016). Rehman FU, Nadeem S, Rehman HU, Haq RU. Thermophysical analysis for three-dimensional MHD stagnation-point flow of nano-material influenced by an exponential stretching surface. Results in physics. 2018 Mar 1; Vol. 8, pp.316-23.
[9]. Khalili, Noran Nur Wahida, Abdul Aziz Samson, Ahmad Sukri Abdul Aziz, and Zaileha Md Ali. "Chemical reaction and radiation effects on MHD flow past an exponentially stretching sheet with heat sink." *Journal of Physics: Conference Series,* vol. 890, Issue no. 1, pp. 012025. IOP Publishing, 2017.
[10]. Ur Rehman F, Nadeem S. Heat transfer analysis for three-dimensional stagnation-point flow of water-based nanofluid over an exponentially stretching surface. *Journal of Heat Transfer*. 2018 May 1, Vol.*140*, Issue 5, pp.052401-1 to 7.
[11]. Khan WA, Irfan M, Khan M. An improved heat conduction and mass diffusion models for rotating flow of an Oldroyd-B fluid. *Results in physics.* 2017 Jan 1; Vol. *7*, pp.3583-9.
[12]. Saleem S, Al-Qarni MM, Nadeem S, Sandeep N. Convective heat and mass transfer in magneto Jeffrey fluid flow on a rotating cone with heat source and chemical reaction. *Communications in Theoretical Physics*. 2018 Nov; Vol. *70*, Issue 5, pp.534.
[13]. Rehman FU, Nadeem S, Rehman HU, Haq RU. Thermophysical analysis for three-dimensional MHD stagnation-point flow of nano-material influenced by anexponential stretching surface. *Results in physics.* 2018 Mar 1, Vol. *8*, pp.316-323.
[14]. Keshtekar, M. M., Khaluei, A., & Fard, H. A. (2014). Effects of thermal radiation, viscous dissipation, variable magnetic field and suction on mixed convection MHD flow of nanofluid over a non-linear stretching sheet. *IOSR journal of Engineering*, *4*, 44-54.
[15]. C. Pang, J.W. Lee, Y.T. Kang, 87: 49-67 (2015). Pang C, Lee JW, Kang YT. Review on combined heat and mass transfer characteristics in nanofluids. *International Journal of Thermal Sciences*. 2015 Jan 1; Vol. *87*, pp.49-67.
[16]. Malvandi A, Hedayati F, Ganji DD. Slip effects on unsteady stagnation point flow of a nanofluid over a stretching sheet. *Powder Technology*. 2014 Feb 1, Vol. *253*, pp.377-84.
[17]. Raju C.S., Saleem S, Mamatha S.U., Hussain I. Heat and mass transport phenomena of radiated slender body of three revolutions with saturated porous: Buongiorno's model. *International Journal of Thermal Sciences.* 2018 Oct 1, Vol. *132*, pp. 309-15.
[18]. Qasim M., Afridi MI, Wakif A, Saleem S. Influence of variable transport properties on nonlinear radioactive jeffrey fluid flow over a disk: utilization of generalized differential quadrature method. *Arabian Journal for Science and Engineering*. 2019 Jun 1, Vol. *44*, Issue 6, pp.5987-5996.
[19]. Upadhya S.M., Raju CS, Shehzad SA, Abbasi FM. Flow of Eyring-Powell dusty fluid in a deferment of aluminum and ferrous oxide nanoparticles with Cattaneo-Christov heat flux. *Powder technology.* 2018 Dec 1, Vol. *340*, pp. 68-76.
[20]. Sheikholeslami M, Ellahi R, Ashorynejad HR, Domairry G, Hayat T. Effects of heat transfer in flow of nanofluids over a permeable stretching wall in a porous medium. *Journal of Computational and Theoretical Nanoscience.* 2014 Feb 1, Vol. *11*, Issue 2, pp. 486-96.
[21]. Raju CS, Hoque MM, Sivasankar T. Radiative flow of Casson fluid over a moving wedge filled with gyrotactic microorganisms. *Advanced Powder Technology*. 2017 Feb 1, Vol. *28*, Issue 2, pp. 575-83.
[22]. Saleem S, Nadeem S, Rashidi MM, Raju CS. An optimal analysis of radiated nanomaterial flow with viscous dissipation and heat source. *Microsystem Technologies*. 2019 Feb 4, Vol. *25*, Issue 2, pp. 683-9.
[23]. Shateyi S, Marewo GT. Numerical solution of mixed convection flow of an MHD Jeffery fluid over an exponentially stretching sheet in the presence of thermal radiation and chemical reaction. *Open Physics*. 2018 Jan 1, Vol. *16*, Issue 1, pp. 249-59.

How to cite this article: Manjula, D. and Jayalakshmi, K. (2019). Multiple Clip conditions on Chemically Reacting Flow of MHD Jeffrey Fluid over Vertical surface in a Suspension of Brownian Motion and Thermophoresis. *International Journal on Emerging Technologies*, *10*(4): 454–464.